Materials Letters 111 (2013) 169–172

Contents lists available at ScienceDirect

Materials Letters

journal homepage: www.elsevier.com/locate/matlet

SiCN-based composite ceramics fabricated by chemical vapor infiltration with excellent mechanical and electromagnetic properties

Fang Ye, Litong Zhang, Xiaowei Yin*, Xiaofei Liu, Yongsheng Liu, Jimei Xue, Laifei Cheng

Science and Technology on Thermostructural Composite Materials Laboratory, Northwestern Polytechnical University, Xi'an 710072, China

ARTICLE INFO

Article history:
Received 8 July 2013
Accepted 20 August 2013
Available online 27 August 2013

Keywords:
SiCN
CVI
Mechanical property
Electromagnetic property

ABSTRACT

A novel SiCN ternary phase was introduced into porous Si_3N_4 preform by chemical vapor infiltration from $SiCl_4$–C_3H_6–NH_3–H_2–Ar, which was used to fabricate Si_3N_4–SiCN composite ceramics. SiCN was composed of amorphous Si_3N_4 matrix and crystalline SiC nano-particles (with a homogeneous size of ~5 nm) uniformly distributed in amorphous matrix. This distinctive microstructure made the Si_3N_4–SiCN ceramics not only maintain a high flexural strength of 227 MPa but realize a low dielectric constant and a high dielectric loss, which led to a minimal electromagnetic wave reflection coefficient of −42.6 dB, ranking the best level in the already-reported structural and wave-absorbing ceramic materials for high-temperature applications.

© 2013 Elsevier B.V. All rights reserved.

1. Introduction

Recently, SiCN has got widespread concerns owing to its combining properties of both SiC and Si_3N_4 [1]. The good tailoring of microstructure, composition and property makes SiCN an important high-temperature material for multifunctional applications [2–4]. For example, SiCN nano-powders synthesized by a laser-induced gas-phase reaction had a higher permittivity and dielectric loss than SiC nano-powders, bulk SiC and Si_3N_4, which can be used to develop more advanced high-temperature electromagnetic (EM) shielding materials [4,5]. However, these SiCN products with good EM property were usually fabricated by powder synthesizing, difficult to form the continuous and compact microstructure, which inhibits their application as matrix materials and the more extensive development of SiCN-based composites with excellent properties.

Chemical vapor infiltration (CVI) is widely used to prepare ceramic matrix with adjustable composition and designable microstructure. Thermodynamic analysis and experimental verification show that a dense and continuous SiCN microstructure can be formed by CVI using $SiCl_4$–CH_4(C_3H_6)–NH_3–H_2–Ar mixture gases [6,7]. To develop the multifunctional properties of CVI SiCN, the detailed studies on its mechanical and EM properties are necessary. In this work, thus, CVI SiCN was introduced into Si_3N_4 preform, and the microstructure, mechanical and dielectric properties of Si_3N_4–SiCN ceramics were investigated.

2. Experimental

The porous Si_3N_4 preform fabricated in the previous work [8] was machined into specimens with dimensions of $3\times4\times40\ mm^3$ and $2.2\times10.15\times22.85\ mm^3$ for flexural strength and dielectric property testing, respectively. They were placed in a CVI reactor to infiltrate SiCN from $SiCl_4$–C_3H_6–NH_3–H_2–Ar system. $SiCl_4$ ($\geq$99.99 wt%), C_3H_6 ($\geq$99.99 wt%) and NH_3 ($\geq$99.99 wt%) were respectively used as silicon, carbon and nitrogen source. H_2 ($\geq$99.999 wt%) was the carrier gas of $SiCl_4$, and Ar ($\geq$99.9 wt%) was used as dilution gas. The processing conditions were as follows: $T=800\ ^\circ C$, $P=1$ kPa, $Q_{SiCl4}:Q_{H2}=0.22$, $Q_{C3H6}:Q_{NH3}=3$, $t=0$, 8, 16 and 24 h. According to the thermodynamic calculation results [7], 800 °C was selected to deposit SiCN in CVI process in order to prepare the more uniform and compact Si_3N_4–SiCN composite ceramics.

The morphology and microstructure of Si_3N_4–SiCN ceramics was observed by scanning electron microscopy (SEM) and transmission electron microscopy (TEM). The chemical composition and chemical bonds of CVI SiCN were examined by X-ray photoelectron spectra (XPS). The flexural strength (σ) was measured via the three-point bending test with a support distance of 30 mm and a loading speed of 0.5 mm/min. The relatively complex permittivity ($\varepsilon_r=\varepsilon'-\varepsilon''j$, ε' is the real part and ε'' is the imaginary part) at frequencies of 8.2–12.4 GHz (X-band) was obtained by a vector network analyzer as shown in Fig. 2d using the waveguide method. The EM absorbing property was discussed by calculating the EM reflection coefficient (*RC*) as follows:

$$\mathrm{RC}=20\log_{10}|\Gamma|,\quad \Gamma=\frac{\sqrt{\frac{\mu_r}{\varepsilon_r}}\tanh(\gamma d)-1}{\sqrt{\frac{\mu_r}{\varepsilon_r}}\tanh(\gamma d)+1},\quad \gamma=\frac{j\omega\sqrt{\mu_r\varepsilon_r}}{c} \tag{1}$$

---

* Corresponding author. Tel.: +86 29 88486068.
E-mail address: yinxw@nwpu.edu.cn (X. Yin).

0167-577X/$ - see front matter © 2013 Elsevier B.V. All rights reserved.
http://dx.doi.org/10.1016/j.matlet.2013.08.082

where γ is the EM wave propagation factor in the material, ω is the angular frequency, c is the speed of light, d is the thickness of material, and μ_r is the relatively complex permeability of material, which was taken as 1 considering the weak magnetic property of composite ceramics in this study.

3. Results and discussion

SEM image (Fig. 1a) shows that porous Si_3N_4 ceramics were composed of rod-like β-Si_3N_4 intercrossing with each other. After CVI, SiCN was infiltrated into the porous preform (Fig. 1b). With the increase of deposition time, more SiCN was introduced into the porous ceramics and the porosity of Si_3N_4–SiCN ceramics gradually decreased (Table 1). Meanwhile, the density and the flexural strength gradually increased (Table 1).

XPS spectrum of CVI SiCN (Fig. 1c) shows that it mainly consisted of Si, C and N elements. Fig. 1d and e are the Si2p and C1s spectra, respectively. They were derived from peak deconvolution and used to analyze the bonding type [10]. In Si2p spectrum, silicon bonded to carbon at 100.8 eV and silicon bonded to nitrogen at 101.6 eV were found. It is noted that no Si–O bond, which should appear at 103 eV, was observed. Thus, O1s peak in Fig. 1c should originate from the absorbed gases, such as CO, CO_2 and H_2O. In C1s spectrum, carbon bonded to silicon at 283.5 eV, free carbon at 284.6 eV and carbon bonded to nitrogen at 286.9 eV were found. According to the previous thermodynamic calculation [7], no free carbon was found in the phase diagram of solid phase products under such preparation conditions, implying the C–C bond may come from the absorbed carbon during testing.

HRTEM image of CVI SiCN (Fig. 1f) shows that nano-sized and spherical particles were uniformly distributed in the continuous and dense matrix phase that exhibited an amorphous state. The nanocrystals had a uniform grain size of ~5 nm. The interplanar spacing of different crystal planes was measured in HRTEM image based on the previous research [11], which corresponded to the (111) plane (0.25 nm) and (200) plane (0.22 nm) of β-SiC, respectively. Combining with the XPS analysis, it can be inferred that CVI SiCN was composed of nano-sized SiC crystals and amorphous Si_3N_4 phase, and nano-sized SiC was uniformly distributed in amorphous Si_3N_4.

The imaginary part of permittivity of the porous Si_3N_4 ceramics was so low that the dielectric loss can be only determined exactly by resonant cavity method [12]. After CVI of SiCN, the permittivity and dielectric loss of Si_3N_4–SiCN ceramics as a function of deposition time in X-band were plotted in Fig. 2. It can be seen that when the deposition time was 8 h, the real part of permittivity of Si_3N_4–SiCN ceramics varied from 4.97 to 4.89 with the imaginary part of permittivity changing from 2.66 to 1.88 at frequencies of 8.2–12.4 GHz. With the deposition time extended to 16 h, the real part of permittivity varied from 6.19 to 5.78 with the imaginary part of permittivity changing from 6.40 to 4.14. Ultimately, when the deposition time reached 24 h, the complex permittivity of Si_3N_4–SiCN ceramics attained the maximum, which varied from 8.10–12.67j to 8.14–11.70j in the testing frequency range. In comparison, the real part of permittivity at 10 GHz (Fig. 2a) of Si_3N_4–SiCN ceramics increased from 4.91 to 8.61 with the imaginary part of permittivity at 10 GHz (Fig. 2b) increasing from 2.15 to 12.54. Because the increase extent of imaginary part was much higher than that of real part, the dielectric loss of Si_3N_4–SiCN ceramics at

Table 1
Mechanical property, density and porosity of Si_3N_4–SiCN composite ceramics.

Materials	Density ($g\ cm^{-3}$)	Porosity (%)	SiCN (vol%)	Flexural strength (MPa)
Si_3N_4	1.906	39.49	0	187
Si_3N_4–SiCN(8 h)	2.048	36.16	3.33	199
Si_3N_4–SiCN(16 h)	2.095	34.90	4.59	216
Si_3N_4–SiCN(24 h)	2.105	34.38	5.11	227

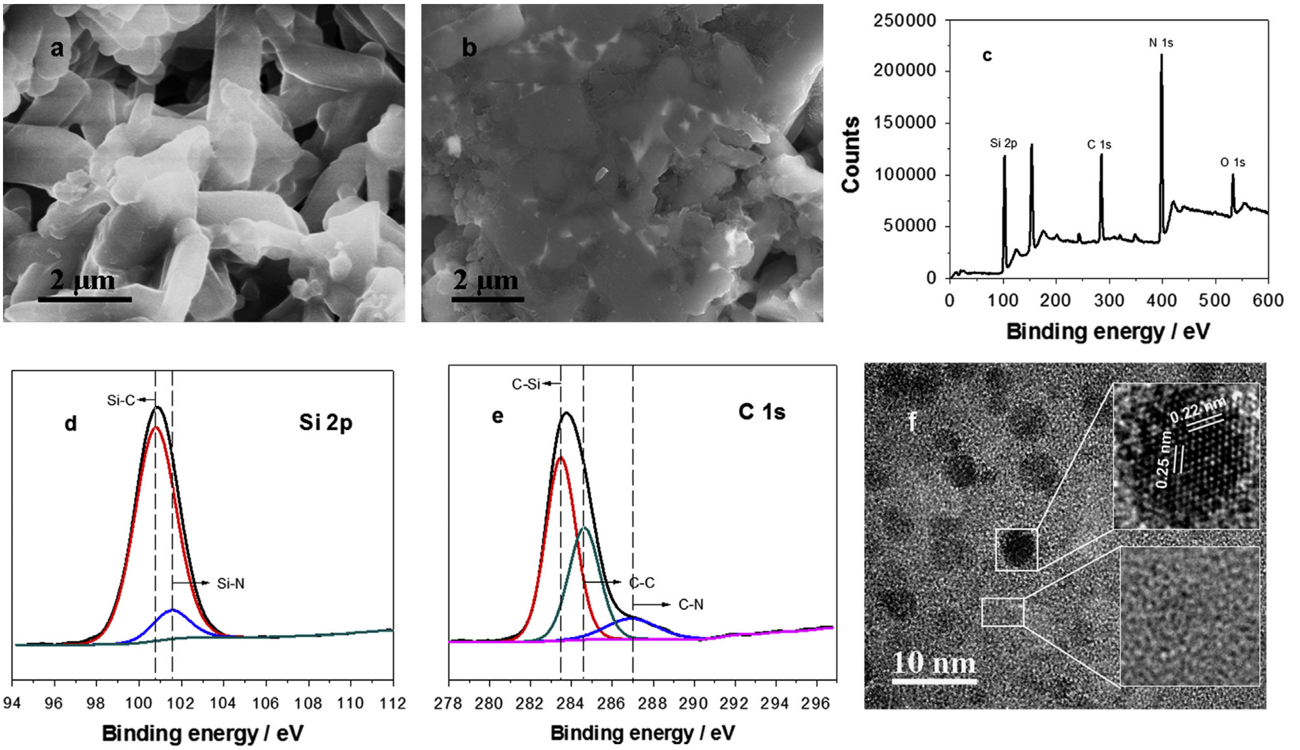

Fig. 1. SEM images of the Si_3N_4 ceramics before (a) and after 8 h infiltration of SiCN (b); XPS survey spectrum (c), deconvolution of the Si2p (d) and C1s peak (e) of CVI SiCN; HRTEM image of CVI SiCN (f).

Download English Version:

https://daneshyari.com/en/article/8021561

Download Persian Version:

https://daneshyari.com/article/8021561

Daneshyari.com